Néel to spin-Peierls transition in a quasi-one-dimensional Heisenberg model coupled to bond phonons

Jason Cornelius Pillay, Keola Wierschem, and Pinaki Sengupta
School of Physical and Mathematical Sciences, Nanyang Technological University, Singapore 637371
(Received 11 April 2013; revised manuscript received 17 July 2013; published 22 August 2013)

The zero and finite temperature spin-Peierls transitions in a quasi-one-dimensional spin-$\frac{1}{2}$ Heisenberg model coupled to adiabatic bond phonons is investigated using the stochastic series expansion (SSE) quantum Monte Carlo (QMC) method. The quantum phase transition from a gapless Néel state to a spin-gapped Peierls state is studied in the parameter space spanned by spatial anisotropy, interchain coupling strength, and spin-lattice coupling strength. It is found that for any finite interchain coupling, the transition to a dimerized Peierls ground state only occurs when the spin-lattice coupling exceeds a finite, nonzero critical value. This is in contrast to the pure 1D model (zero interchain coupling), where adiabatic/classical phonons lead to a dimerized ground state for any nonzero spin-phonon interaction. The phase diagram in the parameter space shows that for a strong interchain coupling, the relation between the interchain coupling and the critical value of the spin-phonon interaction is linear whereas for weak interchain coupling, this behavior is found to have a natural logarithmlike relation. No region was found to have a long range magnetic order and dimerization occurring simultaneously. Instead, the Néel state order vanishes simultaneously with the setting in of the spin-Peierls state. For the thermal phase transition, a continuous heat capacity with a peak at the critical temperature T_c shows a second order phase transition. The variation of the equilibrium bond length distortion δ_{eq} with temperature showed a power law relation which decayed to zero as the temperature was increased to T_c, indicating a continuous transition from the dimerized phase to a paramagnetic phase with uniform bond length and zero antiferromagnetic susceptibility.

DOI: 10.1103/PhysRevB.88.054416 PACS number(s): 75.40.Mg, 75.10.Jm

I. INTRODUCTION

A spin-$\frac{1}{2}$ Heisenberg chain coupled to an elastic lattice is unstable towards dimerization. The cost in elastic energy due to a distortion δ of the lattice ($\sim\delta^2$) is smaller than the accompanying gain in the magnetic energy ($\sim\delta^{4/3}$). This causes the ground state to be stabilized for a lattice with nonzero dimerization[1,2] with a finite spin gap. The transition to such a dimerized phase is known as the spin-Peierls (SP) transition, analogous to the conventional Peierls transition in one-dimensional (1D) metals. In the adiabatic limit, any arbitrarily small coupling to an elastic lattice leads to a dimerized ground state in a spin chain. This is contrary to quantum phonons where quantum lattice fluctuations destroy the bond distortions for small spin-phonon couplings and/or large bare phonon frequencies[3,4]—the transition to a Peierls state occurs only when the spin-phonon coupling exceeds a finite, nonzero critical value (that depends on the bare phonon frequency). The discovery[5] of the quasi-1D inorganic spin-Peierls compound $CuGeO_3$ led to a resurgence in the study of the spin-Peierls transition in low-dimensional spin models. The properties of $CuGeO_3$ have been widely studied within the framework of a 1D spin-$\frac{1}{2}$ Heisenberg model coupled to phonons, with an additional frustrated next-nearest-neighbor interaction.[6]

Further studies have shown that interchain coupling in $CuGeO_3$ is not negligible and is estimated to be $J_\perp/J \approx 0.1$.[7] As such, a more realistic modeling of the real material requires the study of the spin-Peierls transition in 2D or quasi-1D systems. In contrast to spin chains, the ground state of the $S = 1/2$ Heisenberg model in 2D (in the absence of spin-phonon coupling) has long range antiferromagnetic (Néel) order. It is generally believed that even for adiabatic phonons, the spin-phonon coupling has to exceed some nonzero critical value for the ground state to develop a dimerized pattern with a spin gap. What is the nature of the transition? Is there a region in the phase space where the ground state has co-existing dimerization and long range antiferromagnetic order? The existence of several different possible dimerization patterns in 2D means that, in principle, different dimerization patterns can be stabilized for different values of the parameters. Finally, unlike 1D, the Peierls phase in 2D extends to finite temperatures.

The spatially isotropic 2D spin-$\frac{1}{2}$ Heisenberg model with static dimerization patterns has been studied by several authors.[8–13] In these previous works, the energetically most favored dimerization pattern was predicted by comparing the ground state energies for different patterns. Using this same method, the 2D tight binding model with bond distortions[14] and the 2D Peierls-Hubbard model[15–17] have also been studied. In the limit of large on-site repulsion U, the Hubbard model at half filling reduces to the Heisenberg model, thus, results from the Peierls-Hubbard model (in the limit of large U) should be applicable to the present discussion. However, there is no consensus among the different studies as to the nature of the dimerization pattern in the ground state. For the Peierls-Hubbard model at half filling, Tang and Hirsch[15] find a plaquettelike distortion to be energetically favored in the limit of large U. On the other hand, Mazumdar[16] has argued that the minimum energy ground state has a "stairlike" dimerization pattern, corresponding to a wave vector $\mathbf{Q} = (\pi,\pi)$. Zhang and Prelovšek[17] agree with a dimerization pattern with $\mathbf{Q} = (\pi,\pi)$, but conclude that the ground state has dimerization only along one of the axes (staggered dimerized chains, similar to the pattern considered here). For the Heisenberg model

with static dimerization, Al-Omari[12] has concluded that the ground state energy is minimized for a plaquettelike distortion of the lattice which agrees with the conclusion of Tang and Hirsch. On the other hand, Sirker *et al.*[13] find that linear spin wave theory (LSWT) predicts a stairlike dimerization pattern to be most favored, in agreement with Mazumdar. Using LSWT, Sirker *et al.* also find finite regions in the parameter space with co-existing long range magnetic order and nonzero dimerization. However, as pointed out by the authors, results obtained from LSWT are not reliable at large values of dimerization. The effects of interchain coupling was considered early on by Inagaki and Fukuyama[8,9] who studied a quasi-1D system of coupled spin-$\frac{1}{2}$ Heisenberg chains with a fixed dimerization pattern corresponding to a wave vector $\mathbf{Q} = (\pi,0)$. By treating the interchain coupling in a mean-field theory, they were able to map out the ground state phase diagram[8] and study the finite temperature transition[9]. Later, Katoh and Imada[10] studied in detail the nature of the transition. More recently, the effects of impurities have been studied in this model (once again with a mean-field treatment of the interchain coupling) which revealed a region of co-existing Peierls and antiferromagnetic orders.[18–23] In addition to this, the quasi-1D XY model with a $\mathbf{Q} = (\pi,\pi)$ dimerization pattern has recently been studied[24,25] by an extension of the Jordan-Wigner transformation in 2D.[26–28] The effects of quantum phonons in the isotropic 2D model have also been studied,[29] where the authors find that there is no evidence of a transition to the Peierls state for a wide range of values of the bare phonon frequency and the spin-phonon coupling. This is consistent with a previous finding[30] for the same model that the spin wave spectrum along the Brillouin zone boundary is qualitatively similar to that for the pure Heisenberg model.

As can be seen from the discussion above, it can be difficult to uniquely determine the optimal dimerization pattern in a given model. Further, when comparing to experimental results, it is not clear whether the optimal dimerization pattern of a model will be robust to the presence of additional interactions that may occur in the material. Thus, rather than determining the optimum dimerization pattern for a system of weakly coupled Heisenberg chains coupled to bond phonons, we instead choose a fixed dimerization pattern. A natural choice is the stairlike $\mathbf{Q} = (\pi,\pi)$ dimerization pattern that has been experimentally observed in $CuGeO_3$.[31]

In this study, we aim to investigate the SP transition in a spin-$\frac{1}{2}$ quasi-1D Heisenberg antiferromagnet coupled to static $\mathbf{Q} = (\pi,\pi)$ bond phonons. By comparing the elastic energy cost and magnetic energy gain associated with a finite bond distortion at fixed interaction strengths, the complete ground state phase diagram is mapped out in the parameter space of interchain coupling and the strength of spin-lattice interaction. The nature of the Néel-SP quantum phase transition and the evolution of magnetic and Peierls order across the transition are investigated in detail. In the second part of the study, the nature of the thermal transition out of the SP state is investigated—including determination of the universality class—by studying the variation of bond-length distortion and specific heat across the transition.

The rest of the paper is organized as follows. In Sec. II, the model Hamiltonian and the stochastic series expansion (SSE) QMC method used to study it are introduced. The results of the simulations are presented in Sec. III. Section IV concludes with a summary of the results.

II. MODEL AND SIMULATION TECHNIQUES

The stochastic series expansion (SSE) quantum Monte Carlo (QMC) method was used to study a quasi-1D Heisenberg model with spin-phonon coupling. The model is given by the Hamiltonian

$$H = J\sum_{i,j}(1+\lambda u_{i,j})\mathbf{S}_{i,j}\cdot\mathbf{S}_{i+1,j} + \frac{1}{2}K\sum_{i,j}u_{i,j}^2 + J_\perp\sum_{i,j}\mathbf{S}_{i,j}\cdot\mathbf{S}_{i,j+1}, \quad (1)$$

where $J_\perp$ is the interchain coupling, λ is the strength of the spin-phonon coupling (restricted to be only along the chains), $u_{i,j}$'s are the distortions of the bond lengths, and K is the elastic constant for the distortions. Following the experimentally observed[31] dimerization pattern in $CuGeO_3$, the bond length distortions are chosen to be of the form

$$u_{i,j} = (-1)^{i+j}\delta.$$

This amounts to choosing a fixed dimerization pattern along the chains corresponding to the wave vector $\mathbf{Q} = (\pi,\pi)$. The bond distortions can be rescaled by the spin-phonon coupling strength λ, thereby reducing the Hamiltonian to

$$H = \sum_{i,j}(1+(-1)^{i+j}\delta)\mathbf{S}_{i,j}\cdot\mathbf{S}_{i+1,j} + N\delta^2/2\zeta + \alpha\sum_{i,j}\mathbf{S}_{i,j}\cdot\mathbf{S}_{i,j+1}, \quad (2)$$

where $\zeta = \frac{\lambda^2 J}{K}$, $\alpha = J_\perp/J$, and N is the size of the lattice. The static approximation for the displacements makes the computational task easier for the ground state determination since one needs to minimize only the total energy. The following strategy is adopted. The simulations are carried out for the spin variables for several different $\{\alpha,\delta\}$ parameter sets. This produces the spin energy of the system as a function of δ for a fixed α. Next the elastic energy with a particular ζ is added and the total energy is minimized to obtain the value of the ground state distortion for the given set of parameters $\{\alpha,\zeta\}$. This is repeated for different sets of $\{\alpha,\zeta\}$ to obtain the ground state phase diagram in the parameter space spanned by α and ζ.

The above approach fails for the finite temperature studies, where one needs to minimize the free energy (the entropic contribution is nonzero at finite T). Instead, both the equilibrium bond distortion and spin configurations are dynamically determined by Monte Carlo updates. The stochastic series expansion (SSE) QMC method has been used to sample spin configurations in the present model. The SSE method[32–34] is a finite-temperature quantum Monte Carlo method based on importance sampling of the diagonal elements of the Taylor expansion of $e^{-\beta H}$, where β is the inverse temperature $\beta = J/T$. Ground state expectation values can be obtained using sufficiently large values of β, and there are no approximations beyond statistical errors. The use of loop updates[34,35] makes

it possible to explore the spin configuration space of the Hamiltonian (2) in an efficient manner.

To sample the equilibrium bond distortion, we use a straightforward implementation of the Metropolis Monte Carlo algorithm.[36] In order to simplify the bond update, we separate the elastic term $\epsilon(\delta) = N\delta^2/2\zeta$ from the spin-dependent portion of the Hamiltonian. By the linear property of the trace, the partition function then becomes $e^{-\beta\epsilon(\delta)}\mathrm{Tr}(e^{-\beta[H-\epsilon(\delta)]})$. Treating the spin-dependent portion of the Hamiltonian with the SSE method,[32] configuration weights thus become $e^{-\beta\epsilon(\delta)}W(\alpha,\delta,S)$, where W is the weight of the spin configuration S generated by the spin updates (note that W also depends on the Hamiltonian parameters α and δ). During the bond update, a new value of δ is randomly chosen from a discretized grid: $\delta' = \delta \pm \Delta$, where $\Delta = 0.01$ has been used in the present implementation. The proposed move is then accepted with probability

$$\mathrm{Min}\left[1, \frac{e^{-\beta\epsilon(\delta')}}{e^{-\beta\epsilon(\delta)}}\frac{W(\alpha,\delta',S)}{W(\alpha,\delta,S)}\right]. \quad (3)$$

The weights W are easily calculated within the SSE framework, so we do not include them here.

For a static dimerization pattern, the above update simply amounts to sampling δ, the bond distortion parameter. A single Monte Carlo move thus changes the bond distortion of the entire lattice simultaneously. This acts as a global update, and no critical slowing down is expected. Examination of autocorrelation times confirms this intuitive picture. On the other hand, if every bond is updated separately (crucial for determining the optimal dimerization pattern for a model), such a strategy would lead to long autocorrelation times. Instead, one needs to use a more sophisticated approach[37] in such situations.

III. RESULTS

We begin with the determination of the nature of the ground state for different parameter regimes. For a system of weakly coupled Heisenberg chains, it was shown that the estimates for various observables for a spatially anisotropic system depend nonmonotonically on the system size for square ($L_x = L_y$) geometry.[38] One has to go to rectangular ($L_x \neq L_y$) geometries to obtain monotonic behavior of the numerical results for extrapolating to the thermodynamic limit. This is essentially due to a finite-size gap of the coupled chains that scales as $1/L_x$. Only when this gap is smaller than the energy scale of coupling between chains can we begin to approach the thermodynamic limit. Thus, while square lattices eventually converge to the correct thermodynamic values in the limit of infinite system size, they do so much more slowly than appropriately chosen rectangular lattices. Similar effects are expected in the present model for $\alpha \ll 1$. Hence rectangular lattices with the aspect ratio $L_x = 4L_y$ have been studied, with $L_x = 16$–512. An inverse temperature of $\beta = 8L_x$ was found to be sufficient for the observables to have converged to their ground state values. The interchain coupling is varied over $0.006 \leqslant \alpha < 1$, concentrating in the regime $\alpha < 0.1$.

As discussed earlier, for the determination of the ground state phases, the magnetic energy is calculated for a range of values of the static bond distortion and the elastic energy is added subsequently to determine the total energy. For small values of δ, the leading order finite-size correction to the ground state energy is seen to be $\sim 1/L_x^3$, similar to that observed for the pure 2D Heisenberg model.[33] On the other hand, for large values of δ, when the ground state is expected to be in the spin-Peierls phase, the energy scales exponentially with system size. Close to the critical point, extrapolation to the thermodynamic limit becomes difficult due to crossover effects. Instead, the data from the largest system size studied have been used to map out the phase diagram. Fortunately, the data for the largest system sizes studied are found to be well converged—the fractional difference in the energy for the two largest system sizes studied is $\sim 10^{-5}$. This observed convergence allows for a reliable estimation of ground state properties in the thermodynamic limit based on the data from the largest system size: Any finite-size effects on such estimates are expected to be small.

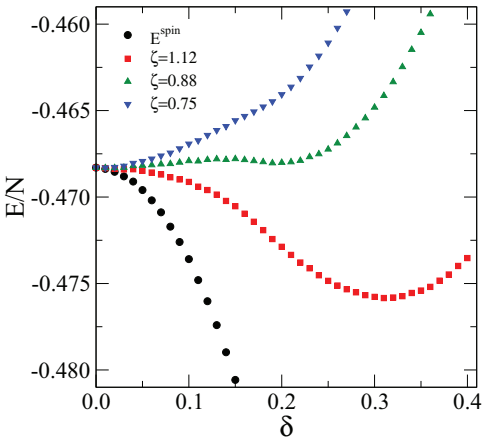

FIG. 1. (Color online) The magnetic (spin) and the total ground state energy per site as a function of the bond distortion for three representative values of the elastic constant ζ and fixed $\alpha = 0.25$. The system size is $N = 256 \times 32$.

The strategy implemented to extract the ground state bond distortion is qualitatively demonstrated in Fig. 1. The total ground state energy is obtained by adding the elastic energy contribution to the spin part of the energy obtained from the simulations. The plot shows the spin part of the energy, as well as the total ground state energy as a function of the bond length distortion δ for three representative values of the elastic energy constant ζ at a fixed value of the interchain coupling ($\alpha = 0.25$). For large ζ, the total energy is minimum for a nonzero value of the bond length distortion δ, which implies a SP ground state. On the other hand, for small ζ, a uniform ground state with $\delta = 0$ is energetically favored. The behavior of the total energy near the critical ζ is also shown. The ground state distortion in bond length is obtained by numerically differentiating the total energy data and solving for $\frac{\partial \mathrm{E}^{\mathrm{tot}}}{\partial\delta}|_{\delta^{gs}} = 0$. In principle, one can also fit a polynomial to the QMC data to get $\mathrm{E}^{\mathrm{spin}}(\delta)$ and add to it the elastic energy term to get $\mathrm{E}^{\mathrm{tot}}(\delta)$. The ground state distortion can then be obtained as a continuous function of δ by solving $\frac{\partial \mathrm{E}^{\mathrm{tot}}}{\partial\delta}|_{\delta^{gs}} = 0$. However, in practice, the numerical minimization is found to be more reliable because of the uncertainty in the order of the polynomial fit.

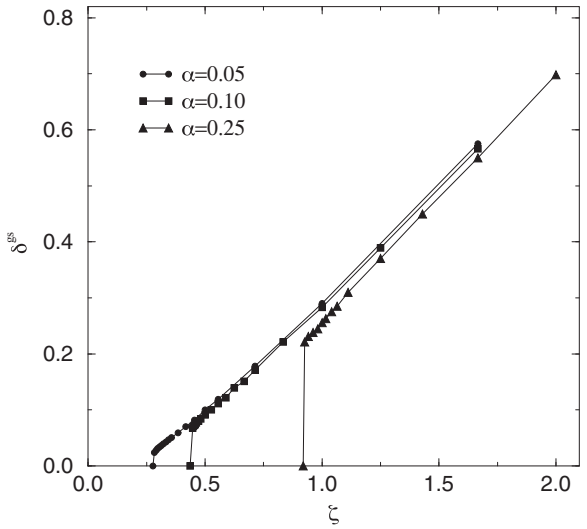

FIG. 2. The equilibrium ground state bond distortion as a function of the spin-lattice coupling for different values of the interchain coupling.

Figure 2 shows the equilibrium distortion in the bond lengths in the ground state of the system as a function of the elastic energy parameter ζ at fixed values of α, obtained as described above. For small values of ζ, the tendency towards dimerization is suppressed, and a uniform (Néel ordered) ground state with uniform bond lengths is stabilized. As ζ is increased above a critical value ζ_c, there is a discontinuous (first order) quantum phase transition to a ground state with a finite, nonzero dimerization. For $\zeta > \zeta_c$, the equilibrium ground state distortion increases monotonically with ζ.

For uncoupled chains with only Heisenberg interaction, the ground state has no true long range magnetic ordering—it is a critical state with algebraically decaying spin-spin correlations. An infinitesimally small ζ is sufficient to destroy the algebraic correlation and the ground state is dimerized for all nonzero spin-phonon coupling. A finite interchain coupling establishes true long range Néel ordering and consequently a finite ζ_c required for a transition to a dimerized ground state. The critical ζ_c increases with increasing interchain coupling.

The results from Fig. 2 are summarized in Fig. 3, which shows the ground state phase diagram for the Hamiltonian (2) in the phase space spanned by the parameters ζ and α. For small ζ and/or large α, the ground state of the system is Néel ordered with zero bond distortion, while for large ζ and/or small α, the ground state is dimerized with a finite spin gap. The critical coupling strength goes to zero as $\zeta_c \sim 1/\ln\alpha$ as $\alpha \to 0$. This is consistent with a similar behavior of the Néel temperature T_N for a system of coupled Heisenberg chains.[39] Since both T_N and ζ_c are approximate measures of the energy required to destroy the Néel ordering, such a similarity in asymptotic behavior is expected. Note that while one could argue that the energy scale of the SP phase (i.e., the spin gap) may also exhibit a dependence on α, it is clear from Fig. 2 that this dependence is very small. Thus, to a first approximation, we do not expect significant corrections to the $1/\ln\alpha$ behavior of the phase boundary described above.

Next we turn to the determination of magnetic properties in the ground state phase with zero bond distortion. This also

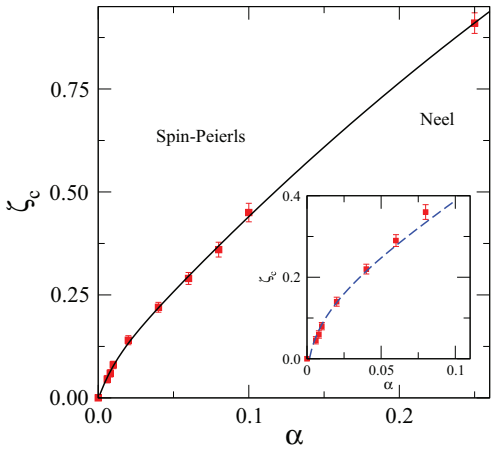

FIG. 3. (Color online) The ground-state phase diagram in the parameter space of the interchain coupling and the spin-lattice coupling strength. The inset shows the results for $\alpha < 0.1$ and the logarithmic dependence of ζ_c as $\alpha \to 0$.

raises the interesting possibility of having a region in the (ζ,α) parameter space where the ground state has co-existing Néel order and nonzero dimerization. Such co-existence has been shown to exist in the presence of doping.[18–23] For this purpose, the static spin susceptibility, defined as

$$\chi(\mathbf{q}) = \frac{1}{N}\sum_{i,j} e^{i\mathbf{q}\cdot(\mathbf{r}_i-\mathbf{r}_j)} \int_0^\beta d\tau \left\langle S_j^z(\tau) S_i^z(0)\right\rangle, \qquad (4)$$

has been studied for the spin part of the Hamiltonian (2) (without the elastic energy term):

$$H = \sum_{i,j} (1+(-1)^{i+j}\delta)\mathbf{S}_{i,j}\cdot\mathbf{S}_{i+1,j} + \alpha\sum_{i,j}\mathbf{S}_{i,j}\cdot\mathbf{S}_{i,j+1}. \qquad (5)$$

If the ground state has long range antiferromagnetic order, the staggered $[\mathbf{Q} = (\pi,\pi)]$ susceptibility scaled by the system size $[\chi(\pi,\pi)/N]$, for a finite system will increase with increasing system size, diverging in the thermodynamic limit. On the other hand, if the ground state has a finite spin gap, $\chi(\pi,\pi)/N$ will vanish in the limit of infinite system size. This qualitative criterion can be expressed in a more quantitative manner by noting that the ground state of the above Hamiltonian undergoes a continuous transition from a Néel ordered state with long range antiferromagnetic order to a spin-gapped, dimerized phase with no long range magnetic order as δ is increased beyond a finite, nonzero critical value δ^* that depends on the interchain coupling α. The transition belongs to the universality class of the 3D Heisenberg model.[40] Finite-size scaling[41] predicts that for such a transition, the finite-size susceptibility at the critical δ scales with the system size as

$$\chi(L_x) \sim L_x^{2-\eta},$$

for a rectangular lattice of dimension $N = L_x \mathrm{x} L_y$. This implies that on a plot of $\chi(\pi,\pi)/L_x^{2-\eta}$, the curves for different system sizes will intersect at the critical δ. The value of the critical exponent η is known to a high degree of accuracy

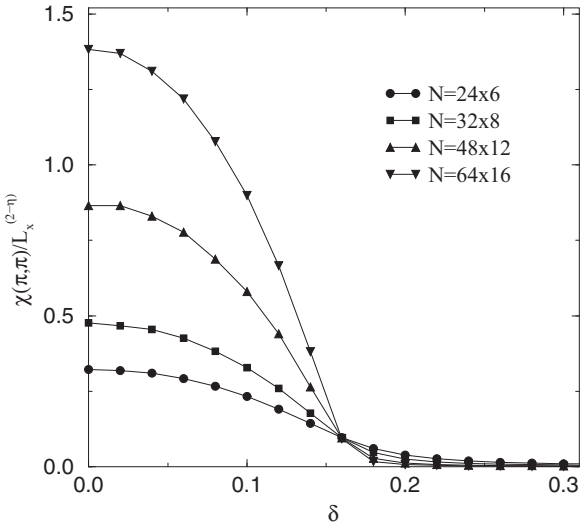

FIG. 4. The ground-state static staggered magnetic susceptibility as a function of bond distortion for a fixed value of the interchain coupling, $\alpha = 0.25$.

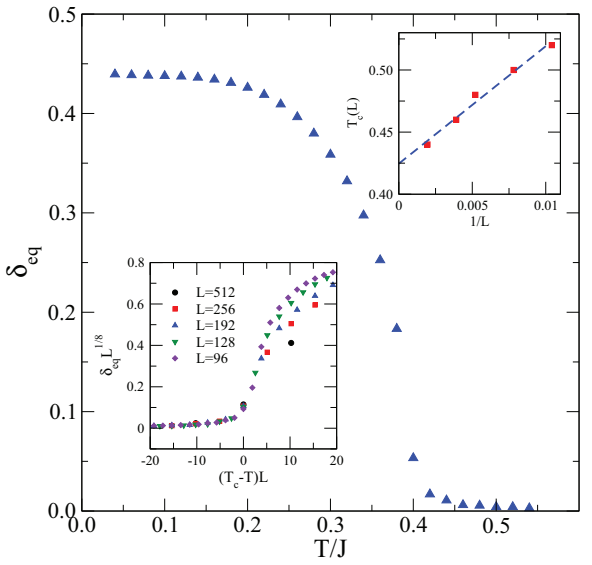

FIG. 5. (Color online) Thermal melting of the SP phase. The main panel shows the evolution of the equilibrium bond distortion as the SP state melts to a normal (paramagnetic) phase. δ_{eq} remains finite at low temperatures, indicating a stable SP ground state. With increasing temperature, the bond length distortion decreases and eventually vanishes via a continuous transition. The data is for a single system size $N = 256 \times 32$ with parameters $\alpha = 0.25$ and $\zeta = 1.14$. The top right inset shows a plot of the $T_c(L)$ finite lattices as a function of the inverse linear dimension to estimate T_c in the thermodynamic limit. The lower left inset shows the data for different system sizes collapse to a single curve close to the transition temperature for 2D Ising critical exponents ($\beta = 1/8$ and $\nu = 1$), confirming the universality class of the transition.

($\eta \approx 0.037$).[42] Figure 4 shows $\chi(\pi,\pi)/L_x^{2-\eta}$ as a function of δ for a fixed value of $\alpha = 0.25$ for several different system sizes. For small δ, the scaled susceptibility increases with increasing system size, indicating the presence of long range magnetic order. For larger values of δ, the scaled susceptibility goes to zero with increasing system size, signaling the opening up of a spin gap. From the data, the critical value of δ is estimated to be $\delta^* \approx 0.16$. This value of the bond length distortion is less than the jump in δ at the transition point ζ_c. This means that for $\zeta > \zeta_c$, the ground state is dimerized with $\delta^{gs} > \delta^*$ and has no long range magnetic order. On the other hand, for $\zeta < \zeta_c$, a uniform ground state is energetically favored that has zero dimerization ($\delta^{gs} = 0$), and long range magnetic order (the Néel state). For no values of ζ is a ground state with $0 < \delta^{gs} < \delta^*$ ever favored energetically. Hence the transition to the dimerized phase is accompanied by the simultaneous vanishing of magnetic order and there is no region of co-existing dimerization and magnetic order. This is true for the present model. Whether it is possible to have ground states with co-existing magnetic order and dimerization in other models (with different dimerization patterns) remains to be seen.

In the final part of the work, we study the thermal phase transitions for the ground state phases determined above. The Néel state in 2D is destroyed by any infinitesimal thermal fluctuations in accordance with the Mermin-Wagner theorem, but the SP phase with a *discrete* broken symmetry persists to finite temperatures. With increasing temperature, the equilibrium bond distortion decreases and finally vanishes at a critical temperature via a thermal phase transition whose nature is probed in detail. We have extended the QMC studies to simulate the Hamiltonian (2) at finite temperatures. As noted in Sec. II, the strategy used to determine the ground state bond distortion fails at finite temperatures because of the nonzero entropic term in the free energy. Instead, both the spin configurations and the bond distortions are evaluated using Monte Carlo updates. Since it breaks a twofold discrete symmetry, the melting of the SP phase is expected to belong to the 2D Ising universality class. Figure 5 (main panel) shows the temperature dependence of the equilibrium bond length distortion δ_{eq} for a single finite-size lattice. The data confirm that the distortion decreases monotonically with T and eventually vanishes at a (size-dependent) critical temperature via a continuous phase transition. The estimate for the true critical temperature in the thermodynamic limit is extracted from a finite-size scaling of the values for a wide range of finite-size systems. The universality class of the thermal transition is verified by plotting $\delta_{eq}(t,L)L^{\beta/\nu}$ vs $tL^{1/\nu}$, where $t = (T_c - T)/T_c$ is the reduced temperature and L is the system size. Close to the transition temperature, the data for different system sizes are found to collapse on a single curve when we use the known critical exponents for the 2D Ising universality class. The calculated specific heat (not shown here) is consistent with the expected 2D Ising universality behavior, but the accuracy was found to be insufficient to extract the critical exponent.

IV. SUMMARY

A quantum Monte Carlo method has been used to study the $S = 1/2$ antiferromagnetic Heisenberg model on a square lattice with varying interchain interaction coupled to static bond phonons. Motivated by experimental observations in the inorganic quasi-1D spin-Peierls compound $CuGeO_3$,[31] the

bond distortions are restricted to be only along the chains, and a single dimerization pattern, with a wave vector $\mathbf{Q} = (\pi,\pi)$, is considered. It is found that in contrast to uncoupled chains, the transition to a dimerized spin-Peierls ground state occurs only when the spin-lattice coupling strength ζ, exceeds a finite, nonzero critical value ζ_c at any nonzero interchain coupling α. For $\zeta < \zeta_c$, the ground state has long range Néel order and zero spin gap, whereas for $\zeta > \zeta_c$, the ground state develops a finite dimerization accompanied by the opening up of a spin gap. The transition is found to be a discontinuous (first order) quantum phase transition. The value of the critical coupling depends on the strength of the interchain coupling and vanishes logarithmically as $\zeta_c \sim 1/\ln\alpha$ as $\alpha \to 0$. The phase diagram in the parameter space of α and ζ is mapped out. Furthermore it is found that in the present model, the transition to the dimerized Peierls state is accompanied by the simultaneous vanishing of magnetic order, and there is no region of co-existing magnetic order and nonzero dimerization. Finally, the thermal transition of the dimerized state is studied in detail and is determined to belong to the 2D Ising universality class.

ACKNOWLEDGMENT

The work was supported in part by grant from the Ministry of Education, Singapore.

[1] E. Pytte, Phys. Rev. B **10**, 4637 (1974).
[2] M. C. Cross and D. S. Fisher, Phys. Rev. B **19**, 402 (1979).
[3] A. W. Sandvik and D. K. Campbell, Phys. Rev. Lett. **83**, 195 (1999).
[4] R. J. Bursill, R. H. McKenzie, and C. J. Hamer, Phys. Rev. Lett. **83**, 408 (1999).
[5] M. Hase, I. Terasaki, and K. Uchinokura, Phys. Rev. Lett. **70**, 3651 (1993).
[6] J. Riera and A. Dobry, Phys. Rev. B **51**, 16098 (1995).
[7] M. Nishi, O. Fujita, and J. Akimitsu, Phys. Rev. B **50**, 6508 (1994).
[8] S. Inagaki and H. Fukuyama, J. Phys. Soc. Jpn. **52**, 3620 (1983).
[9] S. Inagaki and H. Fukuyama, J. Phys. Soc. Jpn. **57**, 1435 (1988).
[10] N. Katoh and M. Imada, J. Phys. Soc. Jpn. **62**, 3728 (1993); **63**, 4529 (1994).
[11] A. Koga, S. Kumada, and N. Kawakami, J. Phys. Soc. Jpn. **68**, 642 (1998); **68**, 2373 (1999).
[12] A. Al-Omari, J. Phys. Soc. Jpn. **69**, 3387 (2000).
[13] J. Sirker, A. Klümper, and K. Hamacher, Phys. Rev. B **65**, 134409 (2002).
[14] Y. Ono and T. Hamano, J. Phys. Soc. Jpn. **69**, 1769 (2000).
[15] S. Tang and J. E. Hirsch, Phys. Rev. B **37**, 9546 (1988).
[16] S. Mazumdar, Phys. Rev. B **36**, 7190 (1987).
[17] F. C. Zhang and P. Prelovšek, Phys. Rev. B **37**, 1569 (1988).
[18] M. Mostovoy, D. Khomskii, and J. Knoester, Phys. Rev. B **58**, 8190 (1998).
[19] M. Saito, J. Phys. Soc. Jpn. **68**, 2898 (1999).
[20] E. Sørensen, I. Affleck, D. Augier, and D. Poilblanc, Phys. Rev. B **58**, R14701 (1998).
[21] A. Dobry, P. Hansen, J. Riera, D. Augier, and D. Poilblanc, Phys. Rev. B **60**, 4065 (1999).
[22] M. Fabrizio, R. Mélin, and J. Souletie, Eur. Phys. J. B **10**, 607 (1999).
[23] R. Mélin, Eur. Phys. J. B **16**, 261 (2000); **18**, 263 (2000).
[24] Y. Ji, J. Qi, J.-X. Li, and C.-D. Gong, J. Phys: Cond. Mat. **9**, 2259 (1997).
[25] Q. Yuan, Y. Zhang, and H. Chen, Phys. Rev. B **64**, 012414 (2001).
[26] Y. R. Wang, Phys. Rev. B **43**, 3786 (1991).
[27] Y. R. Wang, Phys. Rev. B **46**, 151 (1992).
[28] M. Azzouz and C. Bourbonnais, Phys. Rev. B **53**, 5090 (1996).
[29] C. H. Aits and U. Löw, Phys. Rev. B **68**, 184416 (2003).
[30] P. Sengupta, R. T. Scalettar, and R. R. P. Singh, Phys Rev. B **66**, 144420 (2002).
[31] K. Hirota, D. E. Cox, J. E. Lorenzo, G. Shirane, J. M. Tranquada, M. Hase, K. Uchinokura, H. Kojima, Y. Shibuya, and I. Tanaka, Phys. Rev. Lett. **73**, 736 (1994).
[32] A. W. Sandvik, J. Phys. A **25**, 3667 (1992).
[33] A. W. Sandvik, Phys. Rev. B **56**, 11678 (1997).
[34] A. W. Sandvik, Phys. Rev. B **59**, R14157 (1999).
[35] O. F. Syljuåsen and A. W. Sandvik, Phys. Rev. E **66**, 046701 (2002).
[36] N. Metropolis, A. W. Rosenbluth, M. N. Rosenbluth, A. H. Teller, and E. Teller, J. Chem. Phys. **21**, 1087 (1953).
[37] H. Onishi and S. Miyashita, J. Phys. Soc. Jpn. **69**, 2634 (2000).
[38] A. W. Sandvik, Phys. Rev. Lett. **83**, 3069 (1999).
[39] C. Yasuda, S. Todo, K. Hukushima, F. Alet, M. Keller, M. Troyer, and H. Takayama, Phys. Rev. Lett. **94**, 217201 (2005).
[40] S. Chakravarty, B. I. Halperin, and D. R. Nelson, Phys. Rev. Lett. **60**, 1057 (1988); Phys. Rev. B **39**, 2344 (1989).
[41] For a review of finite-size scaling, see: M. N. Barber, in *Phase Transitions and Critical Phenomena*, edited by C. Domb and M. S. Green, Vol. 8 (Academic Press, New York, 1983).
[42] M. Campostrini, M. Hasenbusch, A. Pelissetto, P. Rossi, and E. Vicari, Phys. Rev. B **65**, 144520 (2002).